BIOCHEMISTRY
including biophysical chemistry & molecular biology

ARTICLE

pubs.acs.org/biochemistry

Phosphopeptides Designed for 5-Methylcytosine Recognition

Akiko Nomura[†] and Akimitsu Okamoto[*,†,‡]

[†]Advanced Science Institute, RIKEN, Wako, Saitama 351-0198, Japan

[‡]PRESTO, Japan Science and Technology Agency, 4-1-8 Honcho, Kawaguchi, Saitama 332-0012, Japan

Supporting Information

ABSTRACT: An artificial phosphopeptide has been developed through rational design of the interaction with 5-methylcytosine in duplex DNA. The peptide consists of two tandem zinc finger motifs, in one of which the glutamate was replaced with a phosphotyrosine, the phosphotyrosine in the peptide being effective for methylcytosine selectivity of DNA binding. The flexible modulation of the target methylated sequence by rearrangement of zinc finger peptides is possible, and the phosphopeptide provided us an important hint for expansion of the codes for the interactions of zinc fingers with DNA to methylated DNA sequences. The fluorescence-labeled phosphopeptide provided information on the methylation status of genomic DNA through fluorescence anisotropy after a 10 min incubation.

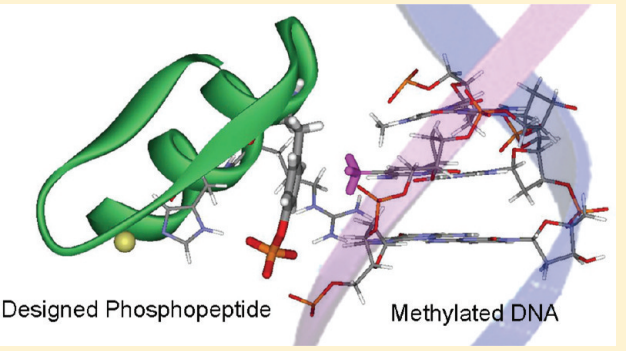

The epigenetic modification of biopolymers independent of their primary sequences effectively regulates gene expression. In particular, cytosine methylation, in which the C5 position of the DNA cytosine base is methylated enzymatically, plays a crucial role in the regulation of chromatin stability, expression control, and genomic imprinting.[1−3] In addition, erroneous DNA methylation may contribute to the etiopathogenesis of tumorigenesis and aging.[4,5] DNA methylation studies still continue to fascinate many chemists, biologists, and physicists, and the literature contains numerous experiments designed to detect efficiently DNA methylation in each research field. However, it is still not easy to distinguish 5-methylcytosine (^{m}C) from cytosine, i.e., to detect the existence of only one methyl group in a long DNA strand. The development of a reaction for the detection of the presence/absence of one methyl group in a DNA strand is a chemically and biologically challenging research subject to contribute to epigenetics research. Several methods have been developed, such as modification-insensitive restriction endonucleases,[6−9] immunoprecipitation,[10−13] bisulfite deamination,[14−16] and osmium complexation.[17−21] One of the biological approaches to fluorescent detection of methylated DNA is to fuse the methyl CpG binding domain (MBD)[22−24] to the enhanced green fluorescent protein (EGFP).[25,26] If a simple organic molecule capable of chemical modification and easy functional addition were to be developed for detection of DNA methylation occurring at a specific sequence without any denaturing or chemical conversion of the sample DNA, i.e., using only a mix-and-read operation, it would contribute to the progress of epigenetic studies.

Addition of a methyl group to cytosine C5 is a small structural change in DNA, although it strongly contributes to the suppression of gene expression. The methyl group of 5-methylcytosine lies hidden in the major groove of the DNA double helical structure. It is not easy to recognize the methyl group sequence-specifically without DNA denaturing. The zinc finger motif, which is one of the major structural motifs involved in eukaryotic protein−nucleic acid interactions, may be the structure most suitable for accessing the DNA major groove in a sequence-specific fashion.[27−30] Two cysteines from the β-sheet region and two histidines from the α-helix coordinate to the zinc ion, and tandemly repeated motifs fit snugly into the major groove of B-DNA.[31,32] The eukaryotic transcription factor Sp1 includes a well-known zinc finger motif,[33,34] which is sometimes chemically modified for DNA binding control.[35−40] The three zinc finger domains of Sp1 can bind with high affinity to a variety of GC box DNA sequences.[41,42] The appropriate chemical modification of Sp1 zinc finger motifs may achieve a new chemical device for sequence-selective methylated DNA detection.

In this study, we report an artificial phosphopeptide developed through rational design of the interaction with 5-methylcytosine in duplex DNA. The phosphotyrosine incorporated into a zinc finger peptide plays an important role in the selective binding ability of the peptide to methylated DNA. A peptide labeled with fluorescence provides information on the methylation status of genomic DNA through fluorescence anisotropy after a short incubation time.

Received: December 24, 2010
Revised: March 6, 2011
Published: March 18, 2011

EXPERIMENTAL PROCEDURES

Materials. *N*-Fluorenylmethoxycarbonyl (Fmoc)-protected *O*-phosphotyrosine (Y_{PO3}), *O*-sulfotyrosine (Y_{SO3}), and 4-nitrophenylalanine (F_{NO2}) were purchased from Novabiochem. The other Fmoc-protected amino acids and reagents used for the peptide autosynthesizer were purchased from Applied Biosystems. Jurkat Genomic DNA, azadC-treated Jurkat Genomic DNA, and CpG methyltransferase (M. *Sss*I) were purchased from New England BioLabs. The alanine-substituted peptides, R22A and K12A, and the target DNA strands were purchased from the Support Unit for Biomaterial Analysis in RIKEN BSI Research Resource Center and Gene Design, Inc., respectively. All other chemicals were of the highest commercial grade available and were used without further purification.

Peptide Synthesis and Characterization. All peptides except K12A and R22A were synthesized on an automatic peptide synthesizer (Model 433A, Applied Biosystems) using the Fmoc solid-phase method on an amide resin (Rink Amide MBHA resin, Novabiochem). After synthesis, the peptides were cleaved from the resin and deprotected by treatment with trifluoroacetic acid/triisopropylsilane/1,2-ethanedithiol/water (94/1/2.5/2.5 v/v) and purified by HPLC on Chemcobond 5-ODS-H (10 × 150 mm, Chemco Scientific). The obtained peptides were characterized by ESI (**1**(F_{NO2})) or MALDI-TOF (the others) mass spectrometry. **1**(E), $[M + H]^+$ calcd, 7220.4; found, 7221.7; **1**(Y), $[M + H]^+$ calcd, 7255.5; found, 7255.9; **1**(Y_{SO3}), $[M + H]^+$ calcd, 7334.6; found, 7334.9; **1**(Y_{PO3}), $[M + H]^+$ calcd, 7335.5; found, 7335.3; **1**(F_{NO2}), $[M]^+$ calcd, 7283.5; found, 7284.0; **2**(Y), $[M + H]^+$ calcd, 7119.2; found, 7119.2; **2**(Y_{PO3}), $[M + H]^+$ calcd, 7199.2; found, 7199.6; **3**(Y), $[M + H]^+$ calcd, 7232.3; found, 7231.6; **3**(Y_{PO3}), $[M + H]^+$ calcd, 7312.3; found, 7312.6.

Fluorescence-Labeled Peptide. *N*-Fmoc-6-aminohexanoic acid (12.4 mg, 35 μmol), (benzotriazol-1-yloxy)tripyrrolidinophosphonium hexafluorophosphate (PyBOP, 18.2 mg, 35 μmol), and 1-hydroxybenzotriazole (HOBt, 4.7 mg, 35 μmol) were dissolved in 0.5 mL of *N*,*N*-dimethylformamide (DMF) and mixed with *N*,*N*-diisopropylethylamine (DIEA, 12.2 mL, 70 μmol). The resin (100 mg) after synthesis of **1**(Y_{PO3}) without cleavage or deprotection of residues was added to the solution, and the mixture was stirred for 1 h at 25 °C. After reaction, the Fmoc group was removed by 20% piperidine in DMF. HOBt (1.9 mg, 14 μmol) and 5 (and 6)-carboxyfluorescein succinimidyl ester (6.6 mg, 14 μmol) were dissolved in 0.5 mL of DMF and mixed with DIEA (4.9 mL, 28 μmol). The solution was added to the resin and stirred in the dark for 12 h at 25 °C. The labeled peptide was cleaved from the resin, deprotected, and then purified as described above. MALDI-TOF, $[M + H]^+$ calcd, 7806.9; found, 7805.6.

Gel Mobility Shift Assays. The DNA strands used in the assay were as follows: for **1**(X), G-strand, ^{32}P-5′-TTT ATA TTA AAT ATT ATG GGG [C/^{m}C]GG GGC CAA TAT ATT A-3′; C-strand, 5′-TAA TAT ATT GGC CC[C/^{m}C] GCC CCA TAA TAT TTA ATA TAA A-3′; 7.02 promoter β region 205−226 of monkey DNA, G-strand, ^{32}P-5′-AGA GTG GGG [C/^{m}C]GG GGC GGA GAG T-3′; C-strand, 5′-ACT CTC CGC CC[C/^{m}C] GCC CCA CTC T-3′; c-Ha-ras promoter region 391−416 of human DNA, G-strand, ^{32}P-5′-GAC GGG CGC GGG G[C/^{m}C]G GGG CGT GCG CA-3′; C-strand, 5′-TGC GCA CGC CC[C/^{m}C] GCC CCG CGC CCG TC-3′; for **2**(X), G-strand, ^{32}P-5′-TTT ATA TTA AAT ATT ATG [C/^{m}C]GG CGT AAT ATA TTA-3′; C-strand, 5′-TAA TAT ATT ACG C[C/^{m}C]G CAT AAT ATT TAA TAT AAA-3′; for **3**(X), G-strand, ^{32}P-5′-TTT ATA TTA AAT ATT ATT GGG [C/^{m}C]GG AAT ATA TTA-3′; C-strand, 5′-TAA TAT ATT C[C/^{m}C]G CCC AAT AAT ATT TAA TAT AAA-3′ (underlines, the sequences to be recognized by the peptide). The ^{32}P-labeled G-strand was annealed with the unlabeled complementary C-strand. The reaction mixture containing the hybridized DNA (50 pM, 500 cpm) and the zinc finger peptide (0−10 μM) was incubated in 20 mM Tris-HCl (pH 8.0), 100 mM sodium chloride, 100 μM zinc chloride, 1 mM tris (2-carboxyethyl)phosphine (TCEP), 0.05% Nonidet P-40, 5% glycerol, 40 ng/μL bovine serum albumin, and 100 ng/μL poly(dI-dC) for 30 min at 4 °C. The reaction mixture was analyzed by polyacrylamide gel electrophoresis in Tris-borate buffer (pH 8.3) at 4 °C. The bands were visualized by autoradiography and quantified using Image Gauge version 4.01 software (Fujifilm). The dissociation constant (K_d) of the peptide for the target DNA was evaluated by curve-fitting the band intensities to the equation $F = [P]/([P] + K_d)$, where F and $[P]$ represent the fraction of the peptide-bound DNA and the total peptide concentration, respectively.

Fluorescence Anisotropy. To prepare pUC(GC), the *Eco*RI-*Bam*HI fragment containing the sequences recognized by fluorescence-labeled 1(Y_{PO3}) (5′-GAT CTT TTA TAT TAA ATA TTA TGG GGC GGG GCC AAT ATA TTA T-3′ and 5′-AAT TAT AAT ATA TTG GCC CCG CCC CAT AAT ATT TAA TAT AAA A-3′, the recognition sequence is shown in underlined nucleotides.) was inserted into pUC19. The methylated pUC(GC) were prepared by treatment with M. *Sss*I.

Fluorescence anisotropy was examined using a Berthold Mithras LB 940. The sample DNA was added to the solution containing the fluorescence-labeled **1**(Y_{PO3}) (50 nM, 50 μL) in 20 mM Tris-HCl buffer (pH 8.0), 100 mM sodium chloride, 20 μM zinc chloride, 1 mM TCEP, and 0.05% Nonidet P-40. The solution was incubated for 10 min at 25 °C. Fluorescence anisotropy was measured at 25 °C. Polarization degree (P) was calculated with the software supplied with the Mithras LB 940. P is determined from measurements of fluorescence intensities parallel ($I_{\parallel}$) and perpendicular ($I_{\perp}$) with respect to the plane of linearly polarized excitation light ($P = (I_{\parallel} - I_{\perp})/(I_{\parallel} + I_{\perp})$). The mP, which is the label of the x axis in Figures 7, 10, and 11, is $P/1000$.

Computational Simulation. The Macromodel 9.0 software package from Schrödinger was used for calculation of the docking structure between the methylated DNA and the zinc finger mutant peptide. The DNA−peptide complex was obtained by modification of the DNA−Zif268 complex (PDB ID: 1AAY) from the Protein Data Bank. All of the amino acids interacting with the target DNA in the third finger of Zif268 were replaced by the corresponding amino acids in the second finger of Sp1. A methyl group was added to the cytosine of CpG in the target DNA. The obtained DNA−peptide complex was modeled using standard parameters supplied with the software package. The side-chain structures of the replaced amino acids were simulated by a conformational search program in water at 298 K, and then the energy of the DNA−peptide complex was minimized at 298 K using an OPLS2001 force field and default parameters of the software package.

CD Spectroscopy. Circular dichroism (CD) spectra were obtained using a Jasco J-720. Measurements were carried out in 10 mM Tris-HCl buffer (pH 7.5) containing 50 mM sodium

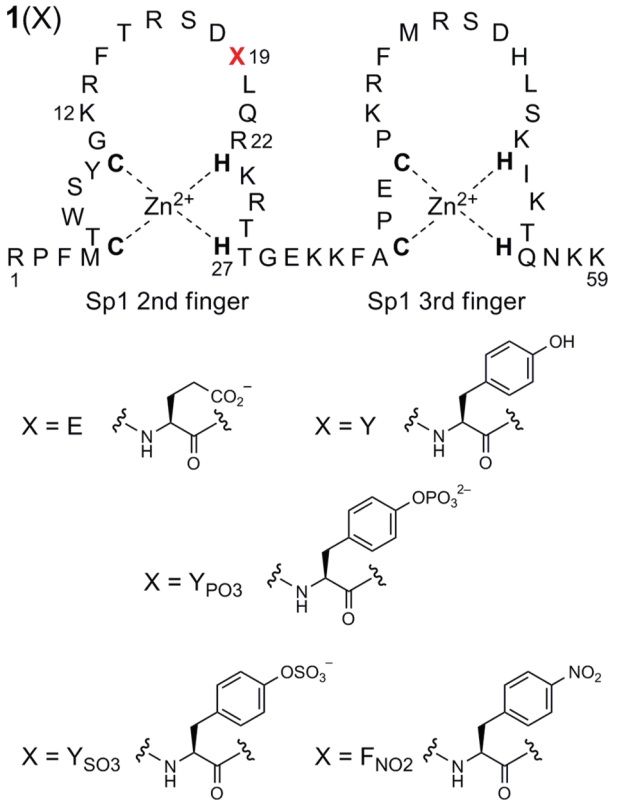

Figure 1. Amino acid sequences of zinc finger peptides **1**(X).

chloride and 0.1 mM TCEP in a capped 1 mm path-length cell at 4 °C under nitrogen. CD intensities were expressed as mean residue ellipticities (deg cm^2 mol^{-1}) calculated by $[\theta] = \theta/lcn$, where θ is the ellipticity observed (mdeg), l is the path length of the cell (cm), c is the peptide concentration (M), and n is the number of peptide bonds in the sequence.

UV−vis Absorption Spectroscopy. UV−vis absorption spectra were recorded on a Shimadzu UV-2550 at 20 °C in 10 mM Tris-HCl buffer (pH = 7.5) containing 50 mM sodium chloride and 300 μM cobalt chloride in a capped 1 cm path-length cell under nitrogen.

^{31}P NMR Spectroscopy. Phosphorus NMR spectra were recorded at 298 K on a JEOL ECA600 NMR spectrometer operating at 242.95 MHz for ^{31}P with ^{1}H decoupling. Phosphorus chemical shifts were referenced to 85% phosphoric acid as an external reference at 0.0 ppm. The peptide samples (1 mM) were dissolved in D_2O/H_2O (90/10) containing 20 mM Tris-HCl (pH = 8.0), 100 mM sodium chloride, and 1 mM dithiothreitol. The typical spectrometer conditions for ^{31}P NMR experiments were as follows: 45° pulse width, 6.25 ms; acquisition time, 0.54 s; sweep width, 30 488 Hz; relaxation delay, 1.5 s; number of acquisitions, 12 000; memory size, 16K; line broadening, 2.0 Hz.

RESULTS AND DISCUSSION

Molecular Design. The Sp1 zinc finger motif was adopted for rational design of a 5-methylcytosine-recognizing peptide in this study because it has been well established chemically and biologically and often used as a scaffold for chemically modifiable peptides. However, the Sp1 zinc finger has never been applied to binding selectively to methylated DNA. The peptide inherently

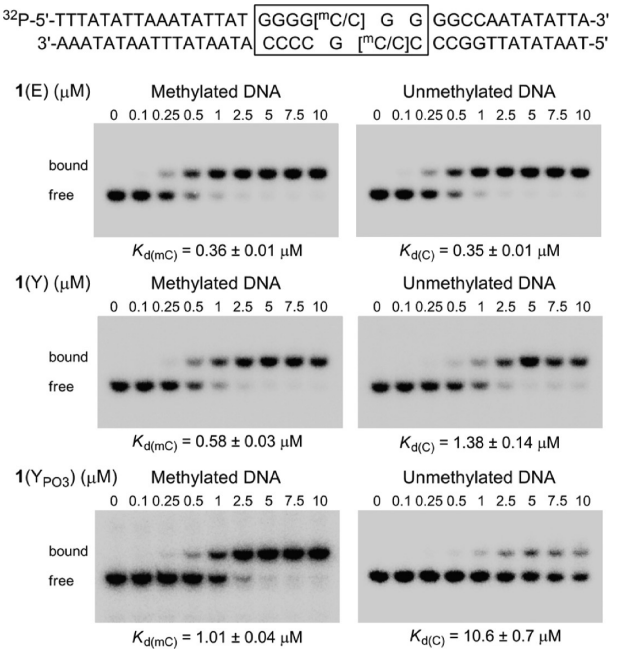

Figure 2. Gel mobility shift assay of ^{32}P-labeled duplex DNA. The mixture containing DNA (50 pM) and the zinc finger peptide (0−10 μM) was incubated in 20 mM Tris-HCl (pH = 8.0), 100 mM sodium chloride, 100 μM zinc chloride, 1 mM tris(2-carboxyethyl)phosphine (TCEP), 0.05% Nonidet P-40, 5% glycerol, 40 ng/μL bovine serum albumin, and 100 ng/μL poly(dI-dC) for 30 min at 4 °C. The box in the DNA sequence is a **1**(E) recognition site.

binds to a CpG sequence in DNA without distinguishing a methylated cytosine from an unmethylated cytosine. A glutamate, which is the third amino acid in the α-helix of the Sp1 second finger, is located at a position enabling recognition of the middle cytosine position of the 3-base pair GCG sequence; however, the side chain of the glutamate does not come within interacting distance of any base of DNA.

We found a hint for molecular design from the sequence of a DNA methylation-dependent transcriptional repressor, Kaiso.[43−45] Kaiso and its families, ZENON and Kaiso-like 1, are suggested to recognize 5-methylcytosine of methylated CpG using their zinc finger motifs, and they have a tyrosine as the third amino acid in the α-helix of the $\beta\beta\alpha$ zinc finger structure.[46] On the basis of this knowledge, replacement of the glutamate of Sp1 with tyrosine or its derivatives may be effective for methylation recognition by the Sp1 zinc finger. We planned the replacement of the glutamate with tyrosine and its common derivative, phosphotyrosine.

Synthesis and Selective Binding to Methylated DNA. The substituted zinc finger peptides were prepared by the conventional Fmoc solid-phase synthesis (Figure 1). The tandem zinc finger peptides consisting of 59 amino acids were designed to reach DNA binding abilities high enough to estimate them because the DNA binding ability of a single zinc finger motif is very low. The synthetic peptides **1**(Y) and **1**(Y_{PO3}) were the tandem of the Sp1 second and third fingers, where tyrosine or phosphotyrosine was installed in place of a glutamate, respectively.

The DNA binding abilities of synthetic peptides **1**(Y) and **1**(Y_{PO3}) in the presence of zinc chloride were investigated through gel mobility shift assays using ^{32}P-labeled DNA, and

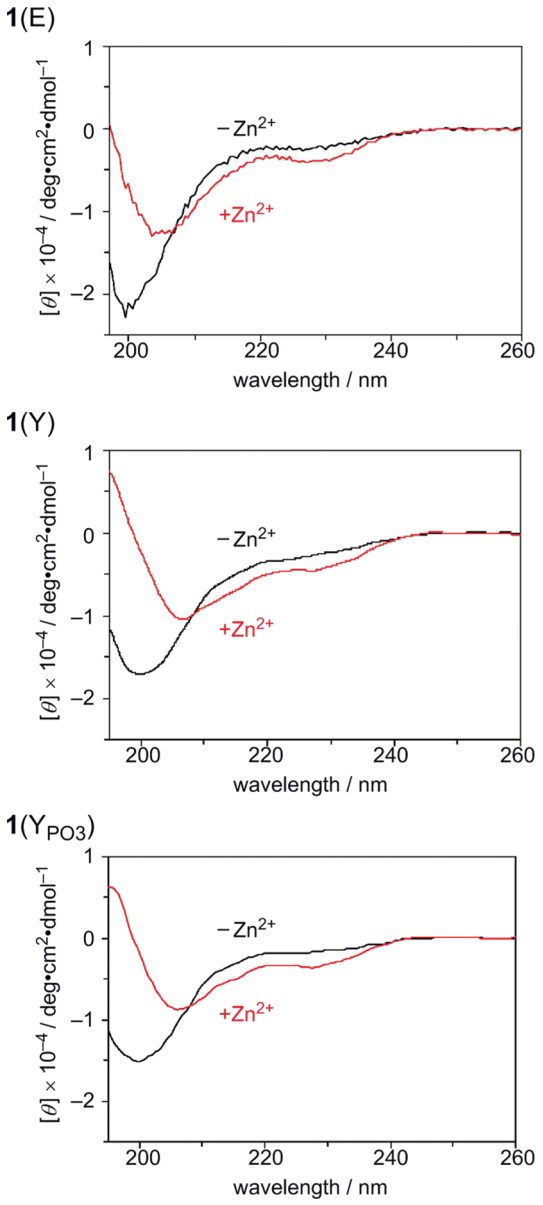

Figure 3. CD spectra of the peptides in the absence (apo forms, black) or presence (zinc finger forms, red) of 3 equiv of zinc chloride. The peptide concentrations were 20 μM for **1**(E) and **1**(Y) and 18 μM for **1**(Y_{PO3}). Measurements were carried out in 10 mM Tris-HCl buffer (pH 7.5) containing 50 mM sodium chloride and 0.1 mM TCEP at 4 °C under nitrogen.

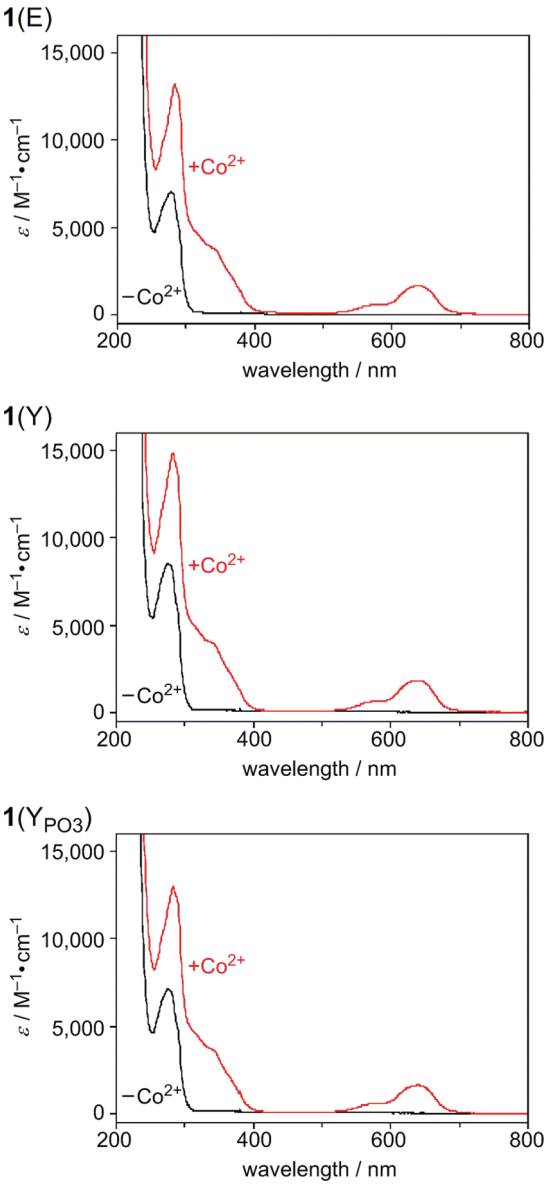

Figure 4. Absorption spectra of the peptides **1**(E) (88 μM), **1**(Y) (80 μM), and **1**(Y_{PO3}) (72 μM) in the absence (apo forms, black) or presence (cobalt complex forms, red) of 300 μM cobalt chloride in 10 mM Tris-HCl buffer (pH = 7.5) containing 50 mM sodium chloride at 20 °C under nitrogen.

compared with that of the peptide with the original sequence **1**(E) (Figure 2). The target DNA duplex included the GGGG-[^{m}C/C]GG sequence, which is known to be recognized by **1**(E).[33,34] Introduction of tyrosine or phosphotyrosine provided high affinity to methylated DNA ($K_{d(mC)}$ = 0.58 ± 0.03 and 1.01 ± 0.04 μM, respectively), although the values of K_d were a little larger than that of **1**(E) (0.36 ± 0.01 μM). On the other hand, introduction of tyrosine or phosphotyrosine resulted in lower affinity for unmethylated DNA. The peptide **1**(Y) showed lower affinity for unmethylated DNA ($K_{d(C)}$ = 1.38 ± 0.14 μM), which was different from **1**(E) ($K_{d(C)}$ = 0.35 ± 0.01 μM). The affinity of the phosphopeptide **1**(Y_{PO3}) for unmethylated DNA drastically decreased ($K_{d(C)}$ = 10.6 ± 0.7 μM). The discrimination factors D_f ($K_{d(C)}/K_{d(mC)}$) of **1**(Y), **1**(Y_{PO3}), and **1**(E) were 2.4, 10.6, and 1.0, respectively, suggesting that the replacement of glutamate with tyrosine derivatives is effective for methylcytosine selectivity of DNA binding.

Maintenance of Zinc Finger Structure. The similar CD and absorption spectra for **1**(Y), **1**(Y_{PO3}), and **1**(E) indicated that these peptides keep the typical structure of zinc finger motifs. The CD spectra of **1**(Y), **1**(Y_{PO3}), and **1**(E) show negative ellipticities at 226 nm and large negative molar ellipticities at 208 nm in the presence of zinc ion (Figure 3). These features are consistent with the presence of regular secondary structure elements and further indicate that the peptides adopt a conformation typical of folded zinc finger domains.[47,48]

The substitution of cobalt ion for the spectroscopically silent (because of its d^{10} configuration) zinc ion is a well-established

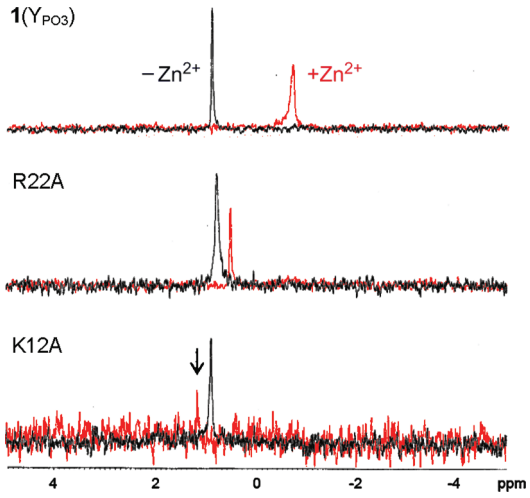

Figure 5. ^{31}P NMR spectra of **1**(Y_{PO3}) and its alanine-substituted peptides (R22A and K12A) at 25 °C. Phosphorus chemical shifts were referenced to 85% phosphoric acid as an external reference at 0 ppm. The peptide samples (1 mM) were dissolved in D_2O/H_2O (90/10) containing 20 mM Tris-HCl (pH = 8.0), 100 mM sodium chloride, and 1 mM dithiothreitol. Black lines, apo forms; red lines, zinc finger forms (in the presence of 3 equiv of zinc chloride).

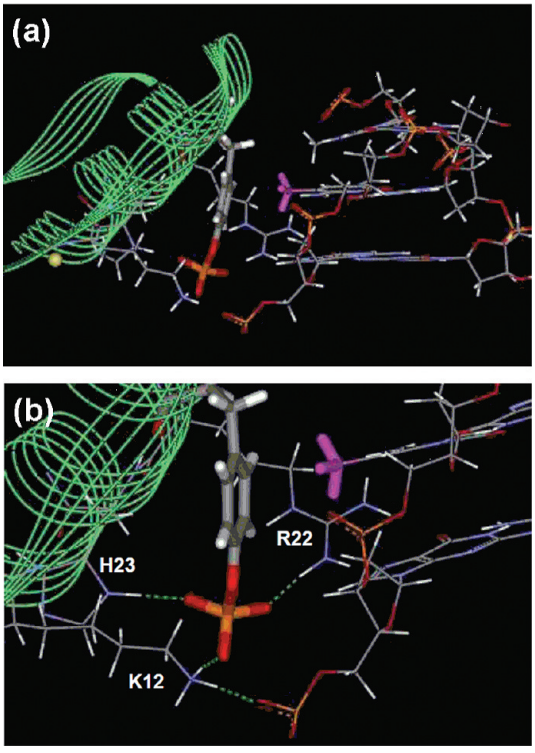

Figure 6. A docking model of the phosphotyrosine-substituted Sp1 second finger region of **1**(Y_{PO3}) and a methylated DNA. (a) Side view. (b) Enlarged view of the area around the phosphate of the phosphotyrosine residue. Dashed lines, hydrogen bonds; sticks, the phosphotyrosine residue (gray, carbon; white, hydrogen; orange, phosphorus; red, oxygen atoms) and the methyl group of 5-methylcytosine (magenta); and yellow sphere, a zinc ion.

technique to probe the coordination environment of zinc-containing metalloproteins.[49−51] The absorption spectra of synthetic peptides exhibited absorption maxima corresponding to the d−d transitions centered around 640 nm with shoulders near 580 nm (Figure 4). The positions and intensities of the d−d transitions were consistent with the formation of typical 1:1 cobalt−peptide complexes with the metal centers occupying tetrahedral or distorted tetrahedral environments for peptides.[52,53]

Phosphate Effect. A phosphopeptide **1**(Y_{PO3}) showed the highest discrimination ability between methylated and unmethylated cytosines among three synthetic peptides; it maintained high binding ability for methylated DNA, whereas the binding ability for unmethylated DNA was about 10-fold lower. The phosphate group in a zinc finger motif seems to play an important role in methylation-selective binding of **1**(Y_{PO3}); thus, the ^{31}P NMR spectrum of **1**(Y_{PO3}) was measured (Figure 5). The spectra exhibited different chemical shifts before and after addition of zinc salt to **1**(Y_{PO3}). The signal of **1**(Y_{PO3}) phosphate moved from 0.90 (apo form) to −0.65 ppm upon addition of zinc salt. The upfield shift in the presence of zinc salt suggests that the **1**(Y_{PO3}) phosphate forms protonation or intramolecular interactions such as hydrogen bonding[54] with spatially adjacent amino acids after the folding of **1**(Y_{PO3}) to the zinc finger structure.

A docking model of the phosphotyrosine-substituted Sp1 s finger region of **1**(Y_{PO3}) and a methylated DNA indicated that the phosphotyrosine of **1**(Y_{PO3}) formed not only a CH−π interaction with the methyl group of 5-methylcytosine (r = 2.79 Å, ω = 105.3°) because the CH−π interaction has been reported to exist between CH bonds and π-electron systems at a distance r < 3.05 Å and an angle ω < 127.5°,[55,56] but also the phosphate of the peptide located within the distance that can form hydrogen-bonding networks with proton-donatable residues K12 (P−O···H−N: 1.58 Å), R22 (1.57 Å), and H23 (1.57 Å) (Figure 6). The shift of the ^{31}P NMR phosphate signal of **1**(Y_{PO3}) may indicate the formation of such an intramolecular interaction.

To evaluate the interaction between the phosphate and the proton-donatable residues, two mutants of **1**(Y_{PO3}) were next prepared, in which K12 or R22 was replaced with an alanine residue (K12A or R22A, respectively), and their ^{31}P NMR spectra were measured. The shifts of the NMR signals observed for both K12A and R22A upon zinc binding were much smaller compared with the result for **1**(Y_{PO3})—from 0.93 to 1.18 ppm for K12A and from 0.82 to 0.55 ppm for R22A (Figure 5)—although they showed CD spectra characteristic of the zinc finger motif as well as **1**(Y_{PO3}). The large shift observed for **1**(Y_{PO3}) phosphate suggests that the phosphate forms hydrogen bonds with K12 and R22. These intramolecular interactions anchoring the phosphotyrosine residue may suppress the conformational fluctuation and determine the location of a CH−π-interactive benzene ring and a phosphate, which are important for methylcytosine-selective binding.

The effect of phosphate on the affinity to the methylated DNA was also investigated by preparation of a series of modified zinc finger peptides, in which the phosphate group was replaced with sulfate or nitro groups capable of being a proton acceptor like phosphate (**1**(Y_{SO3}) and **1**(F_{NO2}), respectively). The folding of **1**(Y_{SO3}) and **1**(F_{NO2}) to a typical zinc finger structure like **1**(Y_{PO3}) in the presence of zinc ion was indicated by their CD and absorption spectra. However, the results obtained from their gel mobility assays were quite different from the case of **1**(Y_{PO3}), exhibiting low binding affinity and low selectivity to methylated DNA (Table 1, $K_{d(mC)}$ = 25.4 ± 1.2 μM and D_f = 0.8 for **1**(Y_{SO3}),

Table 1. K_d Values for Artificial Zinc Finger Peptides to the Target DNA[a]

peptides	$K_{d(mC)}/\mu M$[b]	(n)[c]	$K_{d(C)}/\mu M$[d]	(n)[c]	D_f[e]
1(E)	0.36 ± 0.01	(3)	0.35 ± 0.01	(3)	1.0
1(Y)	0.58 ± 0.03	(3)	1.38 ± 0.14	(3)	2.4
1(Y_{PO3})	1.01 ± 0.04	(6)	10.6 ± 0.70	(4)	10.6
1(Y_{SO3})	25.4 ± 1.2	(3)	21.2 ± 0.9	(3)	0.8
1(F_{NO2})	16.9 ± 1.2	(1)	17.9 ± 1.4	(1)	1.1

[a] Apparent dissociation constants (K_d) were evaluated by curve-fitting the gel band intensities. [b] K_d values for methylated DNA. [c] The number of trials. [d] K_d values for unmethylated DNA. [e] $D_f = K_{d(C)}/K_{d(mC)}$.

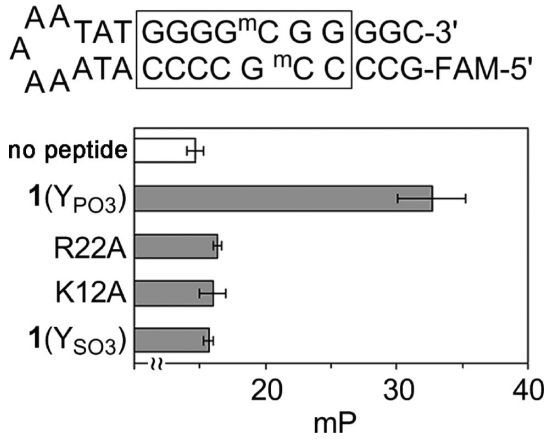

Figure 7. Fluorescence anisotropy of **1**(Y_{PO3}) with 5′-FAM-labeled DNA. A stem-loop DNA, 5′-FAM-GCCC^{m}CGCCCCATAAAAAA-TATGGGG^{m}CGGGGC-3′ (0.2 μM) was added to a solution of peptides, **1**(Y_{PO3}), R22A, K12A, or **1**(Y_{PO3}) (0.2 μM) in a 50 μL solution of 20 mM Tris-HCl (pH 8.0) containing 100 mM sodium chloride, 20 μM zinc chloride, 1 mM TCEP, and 0.05% Nonidet P-40 at 25 °C (n = 3). The box in the DNA sequence is a **1**(Y_{PO3}) recognition site.

$K_{d(mC)}$ = 16.9 ± 1.2 μM and D_f = 1.1 for **1**(F_{NO3})). Replacement of phosphate with a sulfate or nitro group greatly decreased interaction with 5-methylcytosine down to the low level of interaction with unmethylated cytosine. The slight differences of orientation and electronegativity[57] among P−O, S−O, and N−O may affect the intensity of interaction between zinc finger peptides and methylated DNA. The true conformations around a benzene ring induced by the sulfate or nitro groups in **1**(Y_{SO3}) and **1**(F_{NO2}) are still unknown, but the results indicate that their conformations made the methylcytosine-selective CH−π interaction ineffective. The phosphate of **1**(Y_{PO3}) contributes to delicate control of the conformation around the aromatic ring suitable to the CH−π interaction with 5-methylcytosine; the substitution of glutamate of Sp1 second finger with tyrosine derivatives greatly decreased the binding affinity with DNA, whereas only the substitution with phosphotyrosine stopped the large decrease in the binding affinity of the peptide with methylated DNA strands.

Anisotropic analysis, which is one of the effective methods for measuring the binding interaction between peptide and DNA, also showed the effect of the phosphate group on binding with methylated DNA. A fluorescence-labeled stem-loop DNA, of which the stem region has a methylated DNA sequence to be recognized by **1**(Y_{PO3}), 5′-FAM-GCCC^{m}CGCCCCATAAAA-AATATGGGG^{m}CGGGGC-3′, was prepared, and the change in the fluorescence polarization was investigated in the presence of peptides (Figure 7). The addition of **1**(Y_{PO3}) to a solution of the fluorescence-labeled stem-loop DNA induced a large increase in polarization, whereas the addition of K12A and R22A, which lack the intramolecular interactions between the phosphotyrosine residue and the proton donatable residues, exhibited a little change in polarization, suggesting that the binding affinities of these peptides with the methylated DNA are very low. The substitution of a phosphate group with a sulfate group also showed almost the same polarization as that of the fluorescence-labeled DNA in the absence of peptides. The low binding affinity of **1**(Y_{SO3}) with methylated DNA is consistent with the result of the gel mobility shift assays.

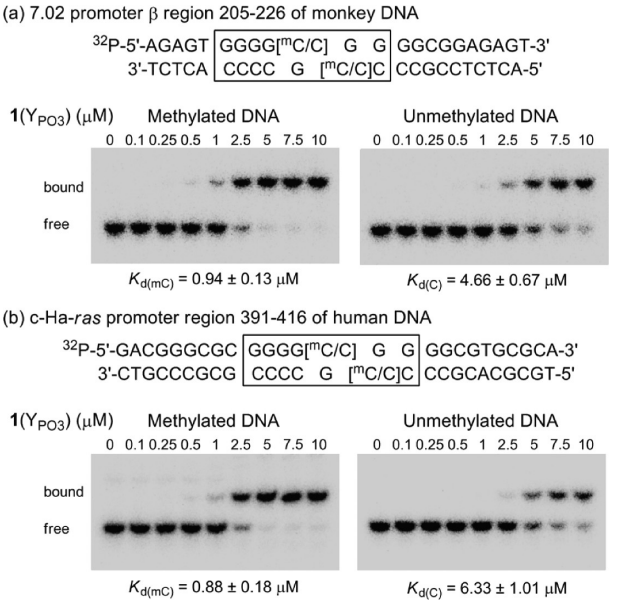

Figure 8. Binding of **1**(Y_{PO3}) to the promoter DNA duplexes including a target region in mixed sequences: (a) 7.02 promoter β region 205−226 of monkey DNA; (b) c-Ha-ras promoter region 391−416 of human DNA.

Binding to Naturally Occurring Sequences. The results presented above show that the phosphopeptide **1**(Y_{PO3}) binds with different affinities for methylated cytosine and unmethylated cytosine sequences. The methylation-selective binding of **1**(Y_{PO3}) is not limited to DNA sequences with high AT-rich flanking sequences. Similar cytosine/methylcytosine sequences with other flanking sequences also showed sufficient selectivity for recognition (Figure 8). We prepared two naturally occurring DNA sequences, the 7.02 promoter β region 205−226 of monkey DNA[58,59] and the promoter region 391−416 of the human Harvey ras proto-oncogene c-Ha-ras1,[60] and tested methylation-selective binding of **1**(Y_{PO3}) with these duplex DNA sequences. The binding abilities of **1**(Y_{PO3}) to these sequences were higher for methylated DNA ($K_{d(mC)}$ = 0.94 ± 0.13 μM for 7.02 promoter and 0.88 ± 0.18 μM for c-Ha-ras promoter) than for unmethylated DNA ($K_{d(C)}$ = 4.66 ± 0.67 μM for 7.02 promoter and 6.33 ± 1.01 μM for c-Ha-ras promoter). The K_d values for methylated DNA were close to that for the model methylated DNA sequence described above, suggesting that the influence of the flanking sequences on binding ability of **1**(Y_{PO3}) with the target methylated sequence is not large.

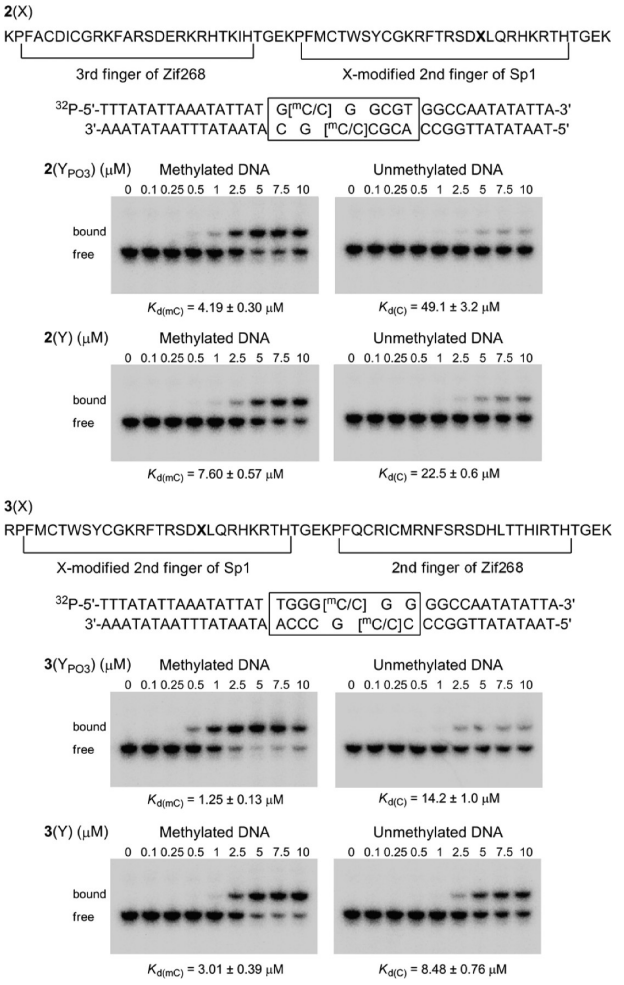

Figure 9. Rearranged tandem zinc finger peptides **2**(X) and **3**(X), their target DNA sequences, and the results of gel mobility shift assays.

Other Combinations of Zinc Finger Motifs. Zinc finger peptides can recognize diverse DNA sequences depending on the combination of zinc finger motifs.[61,62] The flexible modulation of the target sequence by rearrangement of zinc finger motifs is an advantage for extension of the application to detection of various methylation sequences. On the basis of this simple strategy, we designed two types of tandem zinc finger peptides (Figure 9). One of the tandem zinc finger peptides, **2**(X) (X = Y or Y_{PO3}), has the structure that the modified second finger of Sp1 was attached to the *C*-terminus of the third finger of three-zinc finger peptide that contains the DNA-binding domain from the mouse immediate early protein Zif268 consensus binding site,[63,64] which recognizes G[^{m}C/C]GGCGT. Another peptide **3**(X) has the modified Sp1 second finger attached to the *N*-terminus of the Zif268 second finger, which recognizes TGGG-[^{m}C/C]GG. Gel mobility shift assays of phosphopeptides **2**-(Y_{PO3}) and **3**(Y_{PO3}) showed that these peptides selectively bound to their target methylated DNA sequences (D_f = 11.7 for **2**(Y_{PO3}) and 11.4 for **3**(Y_{PO3})). Methylation-selective binding abilities of unphosphorylated peptides **2**(Y) and **3**(Y) were not so high (D_f = 3.0 for **2**(Y) and 2.8 for **3**(Y)) compared with those of phosphopeptides, similar to the methylation-selective binding abilities observed for **1**(Y_{PO3}) and **1**(Y). The rearranged tandem zinc fingers containing the Sp1 second finger substituted with

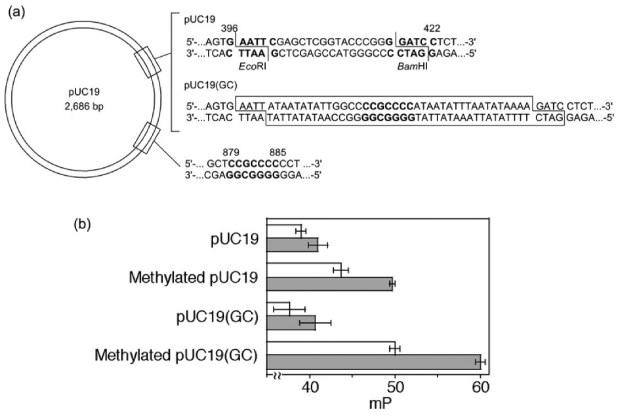

Figure 10. Binding of a zinc finger peptide to methylated plasmid DNA. (a) Sequences of plasmid DNA pUC19 and pUC19(GC). (b) Fluorescence anisotropy of FAM-labeled **1**(Y_{PO3}) with unmethylated and methylated (M. *Sss*I-treated) plasmid DNAs. DNA was added to a solution of FAM-labeled **1**(Y_{PO3}) (0.5 pmol) in a 50 μL solution of 20 mM Tris-HCl (pH 8.0) containing 100 mM sodium chloride, 20 μM zinc chloride, 1 mM TCEP, and 0.05% Nonidet P-40 at 25 °C (n = 3). Bars: white, 0.28 pmol (0.5 μg) DNA; gray, 0.56 pmol (1.0 μg) DNA.

phosphotyrosine exhibited methylation selectivity in the binding to each target sequence. The phosphopeptides will provide us an important hint for expansion of the codes for the interactions of zinc fingers with DNA[65−68] to methylated DNA sequences.

Application to Efficient Methylated DNA Detection. Our designed peptides may also be useful for simple and rapid detection of 5-methylcytosine in a long DNA sequence because of their high binding affinity and selectivity to 5-methylcytosine. A plasmid DNA pUC19 (2686 bp) was adopted as the target DNA of a model experiment because this plasmid originally includes the sequence to which **1**(Y_{PO3}) can bind after methylation, CCGCCCC/GGGGCGG (879−885) (Figure 10). We also prepared a plasmid in which one more CCGCCCC/GGGGCGG sequence was incorporated into a *Bam*H1/*Eco*R1 large fragment of pUC19, pUC19(GC). Unmethylated pUC19 and pUC19(GC) were methylated with a methylase M. *Sss*I, and the methylation was confirmed by checking that the sequence was not cleaved by endonuclease *Sal*I. We also synthesized the zinc finger **1**(Y_{PO3}) labeled with an FAM fluorophore at the *N*-terminus for development of an easy mix-and-read method for methylation detection. This chemically modified peptide was applicable to the anisotropic analysis of unlabeled DNA sequences. We added methylated and unmethylated pUC19 DNA to a solution containing FAM-labeled **1**(Y_{PO3}) and measured the change in the polarization of the emitted polarized light from the FAM excited by polarized light after 10 min incubation. The concentration dependence of polarization was low for unmethylated pUC19, whereas methylated pUC19 showed a larger change in polarization that depended on concentration. Polarization from FAM-labeled **1**(Y_{PO3}) mixed with methylated pUC19(GC), which has two binding sites for **1**(Y_{PO3}), increased by about twice the increment of the polarization observed for methylated pUC19, whereas the polarization observed for unmethylated pUC19(GC) was almost the same low level as that of unmethylated pUC19. The polarization increment of FAM-labeled **1**(Y_{PO3}) well reflected the number of methylated target DNA sequences in the fluorescence anisotropy assay. This methylation sensing assay was performed simply by mixing the

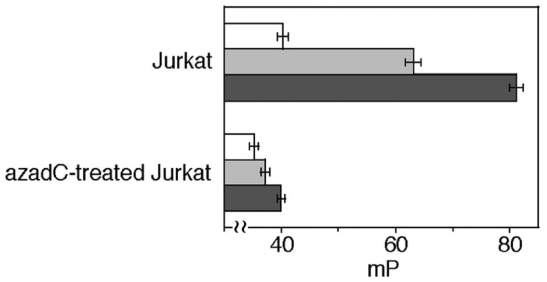

Figure 11. Fluorescence anisotropy of FAM-labeled **1**(Y_{PO3}) with Jurkat DNA. A wild-type DNA or azadC-treated DNA was added to a solution of FAM-labeled **1**(Y_{PO3}) (2.5 pmol) in a 50 μL solution of 20 mM Tris-HCl (pH 8.0) containing 100 mM sodium chloride, 20 μM zinc chloride, 1 mM TCEP, and 0.05% Nonidet P-40 at 25 °C (n = 11). Bars: white, 20 ng of DNA; gray, 60 ng of DNA; black, 100 ng of DNA.

fluorescence-labeled **1**(Y_{PO3}) with the unlabeled DNA and waiting for 10 min. It is in contrast to conventional DNA methylation assays, which usually require at least several hours to operate several complicated pre- or post-treatments, such as denaturing, chemical conversion, rinsing, or sequencing.

Fluorescence anisotropy assay by the use of the FAM-labeled **1**(Y_{PO3}) was also effective for the sensing of methylation in genomic DNA. Human acute T-cell leukemia Jurkat genomic DNA[69,70] exhibited a significant increase in the polarization of **1**(Y_{PO3}) in proportion to the increase in the amount of added DNA (Figure 11). On the other hand, addition of 5-aza-2′-deoxycytidine (azadC)-treated Jurkat DNA[71] often used as a negative control in the study of CpG dinucleotide methylation in the genome produced a small increase in the polarization in the fluorescence anisotropy assay. The methylation detection assay using the FAM-labeled **1**(Y_{PO3}) consists of only mix-and-read operations and exhibited the advantage that DNA methylation can be investigated without denaturing or chemical conversion, in contrast to conventional assays.

In conclusion, we have designed an artificial phosphopeptide capable of sequence-selective binding to methylated DNA. The phosphotyrosine incorporated into an Sp1 zinc finger peptide effectively works for discrimination of a methylated cytosine from an unmethylated cytosine. Target methylated sequences are changeable according to the combination of zinc finger motifs. The new peptide expanded current zinc finger recognition codes to the region of methylated DNA and will make it easy to design molecules that can sense methylated cytosines in epigenetic studies.

■ ASSOCIATED CONTENT

Supporting Information. Detailed experimental data on synthetic protocols, gel shift assay, CD and absorption spectra, and fluorescence anisotropy. This material is available free of charge via the Internet at http://pubs.acs.org.

■ AUTHOR INFORMATION

Corresponding Author

*Phone: +81-48-467-9238. Fax: +81-48-467-9205. E-mail: aki-okamoto@riken.jp.

Funding Sources

This work was supported by a Grant-in-Aid for Young Scientists (B) (#20,750,144) (A.N.) and a Grant-in-Aid for Scientific Research (B) (#20,350,083) (A.O.) from the Japan Society for the Promotion of Science, a Grant-in-Aid for Scientific Research on Priority Areas (Cancer) (#20,014,030) (A.O.) from the Ministry of Education, Culture, Sports, Science, and Technology of Japan (MEXT), and an Incentive Research Grant from RIKEN (A.N.).

■ ACKNOWLEDGMENT

We thank Dr. Hiroyuki Koshino (RIKEN) for running the ^{31}P NMR spectra and the Support Unit for Biomaterial Analysis in RIKEN BSI Research Resource Center for the synthesis of alanine-substituted peptides. We also thank Dr. Takehiro Suzuki (RIKEN) for performing the MALDI-TOF mass spectrometry.

■ ABBREVIATIONS

MBD, methyl CpG binding domain; EGFP, enhanced green fluorescent protein; HPLC, high performance liquid chromatography; MALDI-TOF, matrix-assisted laser desorption ionization/time-of-flight; PyBOP, (benzotriazol-1-yloxy)tripyrrolidinophosphonium hexafluorophosphate; HOBt, 1-hydroxybenzotriazole; DMF, *N*,*N*-dimethylformamide; DIEA, *N*,*N*-diisopropylethylamine; TCEP, tris(2-carboxyethyl)phosphine; CD, circular dichroism; FAM, carboxyfluorescein.

■ REFERENCES

(1) Jones, P. L., and Wolffe, A. P. (1999) Relationships between chromatin organization and DNA methylation in determining gene expression. *Semin. Cancer Biol. 9*, 339–347.

(2) Tate, P. H., and Bird, A. P. (1993) Effects of DNA methylation on DNA-binding proteins and gene expression. *Curr. Opin. Genet. Dev. 3*, 226–231.

(3) Colot, V., and Rossignol, J. L. (1999) Eukaryotic DNA methylation as an evolutionary device. *BioEssays 21*, 402–411.

(4) Jones, P. A., and Laird, P. W. (1999) Cancer epigenetics comes of age. *Nature Genet. 21*, 163–167.

(5) Robertson, K. D. (2005) DNA methylation and human disease. *Nat. Rev. Genet. 6*, 597–610.

(6) Kane, M. F., Loda, M., Gaida, G. M., Lipman, J., Mishra, R., Goldman, H., Jessup, J. M., and Kolodner, R. (1997) Methylation of the hMLH1 promoter correlates with lack of expression of hMLH1 in sporadic colon tumors and mismatch repair-defective human tumor cell lines. *Cancer Res. 57*, 808–811.

(7) Okamoto, A., Tanabe, K., and Saito, I. (2002) Site-Specific Discrimination of Cytosine and 5-Methylcytosine in Duplex DNA by Peptide Nucleic Acids (PNA). *J. Am. Chem. Soc. 124*, 10262–10263.

(8) Nelson, P. S., Papas, T. S., and Schweinfest, C. W. (1993) Restriction endonuclease cleavage of 5-methyl-deoxycytosine hemi-methylated DNA at high enzyme-to-substrate ratios. *Nucleic Acids Res. 21*, 681–686.

(9) Butkus, V., Petrauskiene, L., Maneliene, Z., Klimasauskas, S., Laucys, V., and Janulaitis, A. (1987) Cleavage of methylated CCCGGG sequences containing either N4-methylcytosine or 5-methylcytosine with MspI, HpaII, SmaI, XmaI and Cfr9I restriction endonucleases. *Nucleic Acids Res. 15*, 7091–7102.

(10) Weber, M., Davies, J. J., Wittig, D., Oakeley, E. J., Haase, M., Lam, W. L., and Schubeler, D. (2005) Chromosome-wide and promoter-specific analyses identify sites of differential DNA methylation in normal and transformed human cells. *Nature Genet. 37*, 853–862.

(11) Weber, M., Hellmann, I., Stadler, M. B., Ramos, L., Paabo, S., Rebhan, M., and Schubeler, D. (2007) Distribution, silencing potential and evolutionary impact of promoter DNA methylation in the human genome. *Nature Genet. 39*, 457–466.

(12) Zilberman, D., Gehring, M., Tran, R. K., Ballinger, T., and Henikoff, S. (2007) Genome-wide analysis of Arabidopsis thaliana DNA methylation uncovers an interdependence between methylation and transcription. *Nature Genet. 39*, 61–69.

(13) Jacinto, F. V., Ballestar, E., and Esteller, M. (2008) Methyl-DNA immunoprecipitation (MeDIP): Hunting down the DNA methylome. *BioTechniques 44*, 35–43.

(14) Gonzalgo, M. L., and Jones, P. A. (1997) Rapid quantitation of methylation differences at specific sites using methylation-sensitive single nucleotide primer extension (Ms-SNuPE). *Nucleic Acids Res. 25*, 2529–2531.

(15) Herman, J. G., Graff, J. R., Myöhänen, S., Nelkin, B. D., and Baylin, S. B. (1996) Methylation-specific PCR: A novel PCR assay for methylation status of CpG islands. *Proc. Natl. Acad. Sci. U.S.A. 93*, 9821–9826.

(16) Frommer, M., McDonald, L. E., Millar, D. S., Collis, C. M., Watt, F., Grigg, G. W., Molloy, P. L., and Paul, C. L. (1992) A genomic sequencing protocol that yields a positive display of 5-methylcytosine residues in individual DNA strands. *Proc. Natl. Acad. Sci. U.S.A. 89*, 1827–1831.

(17) Okamoto, A., Tainaka, K., and Kamei, T. (2006) Sequence-selective osmium oxidation of DNA: Efficient distinction between 5-methylcytosine and cytosine. *Org. Biomol. Chem. 4*, 1638–1640.

(18) Tanaka, K., Tainaka, K., Kamei, T., and Okamoto, A. (2007) Direct Labeling of 5-Methylcytosine and Its Applications. *J. Am. Chem. Soc. 129*, 5612–5620.

(19) Tanaka, K., Tainaka, K., Umemoto, T., Nomura, A., and Okamoto, A. (2007) An osmium-DNA interstrand complex: Application to facile DNA methylation analysis. *J. Am. Chem. Soc. 129*, 14511–14517.

(20) Okamoto, A. (2009) Chemical approach toward efficient DNA methylation analysis. *Org. Biomol. Chem. 7*, 21–26.

(21) Nomura, A., Tainaka, K., and Okamoto, A. (2009) Osmium Complexation of Mismatched DNA: Effect of the Bases Adjacent to Mismatched 5-Methylcytosine. *Bioconjugate Chem. 20*, 603–607.

(22) Wade, P. A. (2001) Methyl CpG binding proteins: coupling chromatin architecture to gene regulation. *Oncogene 20*, 3166–3173.

(23) Hendrich, B., and Bird, A. (1998) Identification and characterization of a family of mammalian methyl-CpG binding proteins. *Mol. Cell. Biol. 18*, 6538–6547.

(24) Ohki, I., Shimotake, N., Fujita, N., Nakao, M., and Shirakawa, M. (1999) Solution structure of the methyl-CpG-binding domain of the methylation-dependent transcriptional repressor MBD1. *EMBO J. 18*, 6653–6661.

(25) Kobayakawa, S., Miike, K., Nakao, M., and Abe, K. (2007) Dynamic changes in the epigenomic state and nuclear organization of differentiating mouse embryonic stem cells. *Genes Cells 12*, 447–460.

(26) Stains, C. I., Furman, J. L., Segal, D. J., and Ghosh, I. (2006) Site-specific detection of DNA methylation utilizing mCpG-SEER. *J. Am. Chem. Soc. 128*, 9761–9765.

(27) Wolfe, S. A., Nekludova, L., and Pabo, C. O. (2000) DNA recognition by Cys_2His_2 zinc finger proteins. *Annu. Rev. Biophys. Biomol. Struct. 29*, 183–212.

(28) Pavletich, N. P., and Pabo, C. O. (1991) Zinc finger DNA recognition: Crystal-structure of a Zif268-DNA complex at 2.1-Å. *Science 252*, 809–817.

(29) Nolte, R. T., Conlin, R. M., Harrison, S. C., and Brown, R. S. (1998) Differing roles for zinc fingers in DNA recognition: Structure of a six-finger transcription factor IIIA complex. *Proc. Natl. Acad. Sci. U.S.A. 95*, 2938–2943.

(30) Fairall, L., Schwabe, J. W., Chapman, L., Finch, J. T., and Rhodes, D. (1993) The crystal structure of a two zinc-finger peptide reveals an extension to the rules for zinc-finger/DNA recognition. *Nature 366*, 483–487.

(31) Parraga, G., Horvath, S. J., Eisen, A., Taylor, W. E., Hood, L., Young, E. T., and Klevit, R. E. (1988) Zinc-dependent structure of a single-finger domain of yeast ADR1. *Science 241*, 1489–1492.

(32) Lee, M. S., Gippert, G. P., Soman, K. V., Case, D. A., and Wright, P. E. (1989) Three-dimensional solution structure of a single zinc finger DNA-binding domain. *Science 245*, 635–637.

(33) Kadonaga, J. T., Carner, K. R., Masiarz, F. R., and Tjian, R. (1987) Isolation of cDNA-encoding transcription factor Sp1 and functional-analysis of the DNA-binding domain. *Cell 51*, 1079–1090.

(34) Kriwacki, R. W., Schultz, S. C., Steitz, T. A., and Caradonna, J. P. (1992) Sequence-specific recognition of DNA by zinc-finger peptides derived from the transcription factor Sp1. *Proc. Natl. Acad. Sci. U.S.A. 89*, 9759–9763.

(35) Dhanasekaran, M., Negi, S., and Sugiura, Y. (2006) Designer zinc finger proteins: Tools for creating artificial DNA-binding functional proteins. *Acc. Chem. Res. 39*, 45–52.

(36) Nomura, A., and Sugiura, Y. (2002) Contribution of individual zinc ligands to metal binding and peptide folding of zinc finger peptides. *Inorg. Chem. 41*, 3693–3698.

(37) Nomura, A., and Sugiura, Y. (2004) Hydrolytic reaction by zinc finger mutant peptides: Successful redesign of structural zinc sites into catalytic zinc sites. *Inorg. Chem. 43*, 1708–1713.

(38) Nomura, A., and Sugiura, Y. (2004) Sequence-selective and hydrolytic cleavage of DNA by zinc finger mutants. *J. Am. Chem. Soc. 126*, 15374–15375.

(39) Corbi, N., Libri, V., Fanciulli, M., Tinsley, J. M., Davies, K. E., and Passananti, C. (2000) The artificial zinc finger coding gene 'Jazz' binds the utrophin promoter and activates transcription. *Gene Ther. 7*, 1076–1083.

(40) Nomura, A., and Okamoto, A. (2009) Photoresponsive Tandem Zinc Finger Peptide. *Chem. Commun.* 1906–1908.

(41) Narayan, V. A., Kriwacki, R. W., and Caradonna, J. P. (1997) Structures of zinc finger domains from transcription factor Sp1: Insights into sequence-specific protein-DNA recognition. *J. Biol. Chem. 272*, 7801–7809.

(42) Kadonaga, J. T., Jones, K. A., and Tjian, R. (1986) Promoter-specific activation of RNA polymerase II transcription by Sp1. *Trends Biochem. Sci. 11*, 20–23.

(43) Daniel, J. M., Spring, C. M., Crawford, H. C., Reynolds, A. B., and Baig, A. (2002) The $p120^{ctn}$-binding partner Kaiso is a bi-modal DNA-binding protein that recognizes both a sequence-specific consensus and methylated CpG dinucleotides. *Nucleic Acids Res. 30*, 2911–2919.

(44) Prokhortchouk, A., Hendrich, B., Jørgensen, H., Ruzov, A., Wilm, M., Georgiev, G., Bird, A., and Prokhortchouk, E. (2001) The p120 catenin partner Kaiso is a DNA methylation-dependent transcriptional repressor. *Genes Dev. 15*, 1613–1618.

(45) van Roy, F. M., and McCrea, P. D. (2005) A role for Kaiso-$p120^{ctn}$ complexes in cancer?. *Nat. Rev. Cancer 5*, 956–964.

(46) Daniel, J. M., and Reynolds, A. B. (1999) The Catenin $p120^{ctn}$ Interacts with Kaiso, a Novel BTB/POZ Domain Zinc Finger Transcription Factor. *Mol. Cell. Biol. 19*, 3614–3623.

(47) Adler, A. J., Greenfield, N. J., and Fasman, G. D. (1973) Circular dichroism and optical rotatory dispersion of proteins and polypeptides. *Methods Enzymol. 27*, 675–735.

(48) Johnson, W. C. (1990) Protein secondary structure and circular-dichroism: A practical guide. *Proteins Struct. Funct. Genet. 7*, 205–214.

(49) Chlebowski, J. F., and Coleman, J. E. (1976) Zinc and its role in enzymes. *Metal Ions Biol. Syst. 6*, 1–140.

(50) Bertini, I., and Luchinat, C. (1984) High spin cobalt (II) as a probe for the investigation of metalloproteins. *Adv. Inorg. Biochem. 6*, 71–111.

(51) Maret, W., and Vallee, B. L. (1993) Cobalt as probe and label of proteins. *Methods Enzymol. 226*, 52–71.

(52) Frankel, A. D., Berg, J. M., and Pabo, C. O. (1987) Metal-dependent folding of a single zinc finger from transcription factor-IIIA. *Proc. Natl. Acad. Sci. U.S.A. 84*, 4841–4845.

(53) Green, L. M., and Berg, J. M. (1989) A retroviral Cys-Xaa_2-Cys-Xaa_4-His-Xaa_4-Cys peptide binds metal ions: Spectroscopic studies and

a proposed three-dimensional structure. *Proc. Natl. Acad. Sci. U.S.A. 86*, 4047–4051.

(54) Memissi-Arifi, K., Schmitt, L., Schlewer, G., and Spiess, B. (1995) Complete resolution of the microscopic protonation equilibria of $_D$-myo-inositol 1, 2, 6-tris (phosphate) and related compounds by ^{31}P NMR and potentiometry. *Anal. Chem. 67*, 2567–2574.

(55) Nishio, M., Hirota, M., and Umezawa, Y. (1998) *The CH/π Interaction. Evidence, Nature, and Consequences*, Wiley-VCH, New York.

(56) *r*, perpendicular distance between the hydrogen and the π-plane; *ω*, dihedral angle defined by C_1OC_2 and HC_1C_2 planes; O, center of the π-plane; C_1 and C_2, the nearest and second nearest sp^2-carbons to the hydrogen, respectively.

(57) Aleksovska, S., Petruševski, V. M., and Šoptrajanov, B. (1997) Infrared spectra of the monohydrates of manganese(III) phosphate and manganese(III) arsenate: Relation to the compounds of the kieserite family. *J. Mol. Struct. 408/409*, 413–416.

(58) Dynan, W. S., Saffer, J. D., Lee, W. S., and Tjian, R. (1985) Transcription factor Sp1 recognizes promoter sequences from the monkey genome that are simian virus 40 promoter. *Proc. Natl. Acad. Sci. U.S.A. 82*, 4915–4919.

(59) Dynan, W. S., Sazer, S., Tjian, R., and Schimke, R. T. (1986) Transcription factor Sp1 recognizes a DNA sequence in the mouse dihydrofolate reductase promoter. *Nature 319*, 246–248.

(60) Ishii, S., Kadonaga, J. T., Tjian, R., Brady, J. N., Merlino, G. T., and Pastan, I. (1986) Binding of the Sp1 transcription factor by the human Harvey ras1 proto-oncogene promoter. *Science 232*, 1410–1413.

(61) Liu, Q., Segal, D. J., Ghiara, J. B., and Barbas, C. F., III. (1997) Design of polydactyl zinc-finger proteins for unique addressing within complex genomes. *Proc. Natl. Acad. Sci. U.S.A. 94*, 5525–5530.

(62) Uno, Y., Matsushita, K., Nagaoka, M., and Sugiura, Y. (2001) Finger-positional change in three zinc finger protein Sp1: Influence of terminal finger in DNA recognition. *Biochemistry 40*, 1787–1795.

(63) Christy, B. A., Lau, L. F., and Nathans, D. (1988) A gene activated in mouse 3T3 cells by serum growth factors encodes a protein with "zinc finger" sequences. *Proc. Natl. Acad. Sci. U.S.A. 85*, 7857–7861.

(64) Christy, B., and Nathans, D. (1989) DNA binding site of the growth factor-inducible protein Zif268. *Proc. Natl. Acad. Sci. U.S.A. 86*, 8737–8741.

(65) Choo, Y., and Klug, A. (1994) Toward a code for the interactions of zinc fingers with DNA: Selection of randomized fingers displayed on phage. *Proc. Natl. Acad. Sci. U.S.A. 91*, 11163–11167.

(66) Choo, Y., and Klug, A. (1994) Selection of DNA-binding sites for zinc fingers using rationally randomized DNA reveals coded interactions. *Proc. Natl. Acad. Sci. U.S.A. 91*, 11168–11172.

(67) Segal, D. J., Dreier, B., Beerli, R. R., and Barbas, C. F., III (1999) Toward controlling gene expression at will: Selection and design of zinc finger domains recognizing each of the 5′-GNN-3′ DNA target sequences. *Proc. Natl. Acad. Sci. U.S.A. 96*, 2758–2763.

(68) Sera, T., and Uranga, C. (2002) Rational design of artificial zinc-finger proteins using a nondegenerate recognition code table. *Biochemistry 41*, 7074–7081.

(69) Kochanek, S., Toth, M., Dehmel, A., Renz, D., and Doerfler, W. (1990) Interindividual concordance of methylation profiles in human genes for tumor necrosis factors α and *β*. *Proc. Natl. Acad. Sci. U.S.A. 87*, 8830–8834.

(70) Nedwin, G. E., Naylor, S. L., Sakaguchi, A. Y., Smith, D., Jarrett-Nedwin, J., Pennica, D., Goeddel, D. V., and Gray, P. W. (1985) Human lymphotoxin and tumor necrosis factor genes: structure, homology and chromosomal localization. *Nucleic Acids Res. 13*, 6361–6373.

(71) Christman, J. K. (2002) 5-Azacytidine and 5-aza-2′-deoxycytidine as inhibitors of DNA methylation: mechanistic studies and their implications for cancer therapy. *Oncogene 21*, 5483–5495.